

# Distribution Normalization: An “Effortless” Test-Time Augmentation for Contrastively Learned Visual-language Models

Yifei Zhou <sup>\*1</sup> Juntao Ren <sup>\*1</sup> Fengyu Li <sup>\*1</sup> Ramin Zabih <sup>1</sup> Ser-Nam Lim <sup>2</sup>

## Abstract

Advances in the field of visual-language contrastive learning have made it possible for many downstream applications to be carried out efficiently and accurately by simply taking the dot product between image and text representations. One of the most representative approaches proposed recently known as CLIP (Radford et al., 2021) has quickly garnered widespread adoption due to its effectiveness. CLIP is trained with an InfoNCE loss that takes into account both positive and negative samples to help learn a much more robust representation space. This paper however reveals that the common downstream practice of taking a dot product is only a zeroth-order approximation of the optimization goal, resulting in a loss of information during test-time. Intuitively, since the model has been optimized based on the InfoNCE loss, test-time procedures should ideally also be in alignment. The question lies in how one can retrieve any semblance of negative samples information during inference. We propose Distribution Normalization (DN), where we approximate the mean representation of a batch of test samples and use such a mean to represent what would be analogous to negative samples in the InfoNCE loss. DN requires no retraining or fine-tuning and can be effortlessly applied during inference. Extensive experiments on a wide variety of downstream tasks exhibit a clear advantage of DN over the dot product. Our code is available at <https://github.com/fengyuli2002/distribution-normalization>.

## 1. Introduction

Contrastive Learning (Jaiswal et al., 2020; Chen et al., 2020a; Tian et al., 2020; Chen et al., 2020d; Robinson et al.,

<sup>\*</sup>Equal contribution <sup>1</sup>Cornell University <sup>2</sup>Meta AI. Correspondence to: Yifei Zhou <yz639@cornell.edu>, Ser-Nam Lim <sernamlim@meta.com>.

2020) has become an important area of research in recent years due to its wild success in self-supervised representation learning. The key idea behind contrastive learning is to group positive samples that share similar semantics (e.g., images resulting from applying different augmentations to the same image), while separating semantically different negative samples (e.g., different images with different data augmentations).

On the heels of this progress, contrastive learning has also been shown to be very effective for creating a joint representation space between images and text (Radford et al., 2021; Patashnik et al., 2021; Zhou et al., 2022; Dhariwal & Nichol, 2021). The CLIP approach proposed in (Radford et al., 2021) is at the forefront of this research effort and has been shown to be the state-of-the-art in multiple downstream tasks. The model is generally pre-trained on a large-scale dataset of image-text pairs that form the positive samples, while the negative samples are composed from random pairing of images and text. After the model is trained, it becomes fairly straightforward to perform cross modal retrieval: given an image, its representation from the model can be used to retrieve text representations from the same model and vice versa. Consequently, such a paradigm has similarly opened the doors to state-of-the-art performance in zero-shot classification (Zhai et al., 2021; Jia et al., 2021), cross-modal retrieval (Yu et al., 2022; Lu et al., 2021; Li et al., 2020b; 2019), and evaluation of machine-generated captions (Hessel et al., 2021; Jiang et al., 2019; Lee et al., 2020).

With all the success mentioned, we however observe a “mismatch” between the pre-training objective of such cross-modal representation models and their downstream usage. Most if not all of these models are trained taking into considering of both positive and negative samples, of which one of the most popular optimization objectives is the InfoNCE loss (Sohn, 2016; van den Oord et al., 2018; Zhang et al., 2020). The InfoNCE loss considers negative samples from the data distribution per positive sample and has been shown to be very effective for cross-modal representation learning. In contrast, during test-time, the retrieval is often conducted using the dot product between the query and the gallery, which does not utilize any information in regards to the data

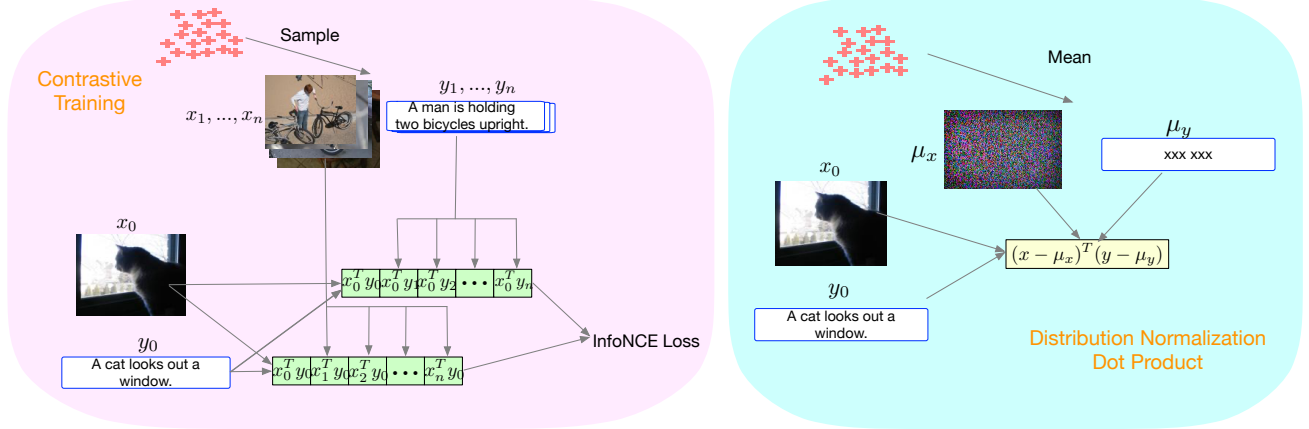


Figure 1. An illustration of how our proposed Distribution Normalization better aligns with the contrastive training objective. Image encoder and Text encoder are omitted for simplicity.

distribution.

This paper presents our findings that rectifying such misalignment can boost performance consistently across a variety of downstream tasks. We particularly analyze the InfoNCE objective and first show that the common practice of taking a dot product is only a zeroth-order approximation. We further show that by approximating the mean of the testing distribution and incorporating it into the similarity measure better approximates the InfoNCE objective used during training. We call our proposed approach Distribution Normalization (DN) – DN is “effortless” to implement and does not require any retraining, fine-tuning or labeled data.

To investigate how this simple modification affects the performance of CLIP and its state-of-the-art variants in practice, we conduct extensive experiments on a wide variety of tasks involving measuring cross-modal similarities, including zero-shot classification, cross-modal retrieval, and evaluation of machine-generated captions. In all the settings that we have studied, DN displays a clear benefit over direct dot product. Our contributions are: (1) We present an insightful analysis of why the dot product as a similarity measure is only a zeroth-order approximation; (2) We propose DN to overcome this shortcoming by utilizing an approximation of the test-time distribution, and also provide guidance on how DN can be effortlessly implemented in practice; (3) We provide extensive supporting empirical evidence as well as ablation studies that demonstrate the fidelity of DN for practical use.

## 2. Background & Related Works

### 2.1. Contrastive Learning

Contrastive learning has become a popular method for self-supervised representation learning, where the goal is to

learn embedding functions such that semantically similar samples are closer in embeddings space while semantically dissimilar samples are embedded further apart (Tian et al., 2019; Wang & Isola, 2020; Peng et al., 2022; You et al., 2021; Yuan et al., 2021; Grill et al., 2020). Among various contrastive learning methods, this paper specifically focuses on the InfoNCE loss, which optimizes the probability of correctly identifying the positive sample (van den Oord et al., 2018), as it has been one of the most frequently used objectives in recent contrastive learning tasks (He et al., 2019; Chen et al., 2020c;a;b).

### 2.2. Learning via Natural Language Supervision

Several recent studies (Chen et al., 2019; Gan et al., 2020; Li et al., 2020a;b) leverage large-scale datasets of image-text pairs to supervise vision-language pre-training (VLP) with a contrastive objective. CLIP (Radford et al., 2021) is one such example that is contrastively trained to create a joint visual-language representation space, which has produced empirical success in downstream tasks such as zero-shot classification and cross-modal retrieval over previous state-of-the-art models (Lu et al., 2021; Wang et al., 2020; Yang et al., 2022; Li et al., 2021). Since CLIP’s introduction, several other works have utilized a similar contrastive objective to create good visual-language representations and achieve state-of-the-art performance on many downstream tasks involving datasets that the model was not pre-trained on (Li et al., 2021; Jia et al., 2021; Chen et al., 2019; Faghri et al., 2017; Kim et al., 2021). For example, ALIGN scales joint pre-training to minimally-filtered datasets (Jia et al., 2021), while ALBEF (Li et al., 2021) and TCL (Yang et al., 2022) focus on learning more semantically meaningful multi-modal interactions. It is noteworthy that these SOTA models all leverage the InfoNCE loss as their key training objective, and apply a simple dot product in

downstream tasks.

### 2.3. Image Caption Evaluation

Image caption evaluation is the task of automatically scoring the quality of a caption given the corresponding image and optionally reference captions. The quality of image caption metrics are evaluated with respect to its correlation with human ratings. While traditional image caption metrics such as BLEU-4 (Papineni et al., 2002), ROUGE-L (Lin, 2004), METEOR (Banerjee & Lavie, 2005), CIDEr (Vedantam et al., 2014), and SPICE (Anderson et al., 2016) evaluate the candidate caption by measuring the n-gram overlap of the candidate with the references, more contemporary neural metrics (Jiang et al., 2019; Yi et al., 2020; Kane et al., 2020; Lee et al., 2020; Cui et al., 2018) judge the candidate caption by comparing the neural embeddings of the caption with that of the image and references, and are much more flexible. Among them, the one most related to our work is CLIPScore (Hessel et al., 2021). By simply passing test image and caption pairs through the pre-trained CLIP image and text encoders and taking the dot product, CLIPScore achieves state-of-the-art performance using only the candidate caption and the corresponding image without the need for references.

## 3. Methodology

This section is organized as follows: in Section 3.1, we show that a dot product is only a zeroth-order approximation of the pre-training objective and how a better approximation arises naturally from the InfoNCE objective, and in Section 3.2, we explain how this idea can be effortlessly implemented in practice.

### 3.1. Analysis of InfoNCE Loss

We start from the original form of InfoNCE loss (Sohn, 2016; van den Oord et al., 2018; Zhang et al., 2020):

$$\begin{aligned} \mathcal{L}_{NCE} = & \mathbb{E}_{x_0, y_0 \sim D} \\ & \mathbb{E}_{y_1, \dots, y_n \sim D} - \log \frac{e^{\phi(x_0)^\top \psi(y_0) / \tau}}{e^{\phi(x_0)^\top \psi(y_0) / \tau} + \sum_{i=1}^n e^{\phi(x_0)^\top \psi(y_i) / \tau}} \\ & - \mathbb{E}_{x_1, \dots, x_n \sim D} \log \frac{e^{\phi(x_0)^\top \psi(y_0) / \tau}}{e^{\phi(x_0)^\top \psi(y_0) / \tau} + \sum_{i=1}^n e^{\phi(x_i)^\top \psi(y_0) / \tau}}, \end{aligned} \quad (1)$$

where  $D$  is the training distribution,  $x_0, y_0$  are images and text belonging to the same pair,  $x_1, \dots, x_n$  and  $y_1, \dots, y_n$  are random images and text in the same batch,  $\phi, \psi$  are image and text encoders respectively, and  $\tau$  is a temperature constant.

InfoNCE loss is equivalent to:

$$\begin{aligned} \mathcal{L}_{NCE} = & \mathbb{E}_{x_0, y_0 \sim D} [\mathbb{E}_{y_1, \dots, y_n \sim D} \log \frac{1}{1 + \frac{\sum_{i=1}^n e^{\phi(x_0)^\top \psi(y_i) / \tau}}{e^{\phi(x_0)^\top \psi(y_0) / \tau}}} \\ & + \mathbb{E}_{x_1, \dots, x_n \sim D} \log \frac{1}{1 + \frac{\sum_{i=1}^n e^{\phi(x_i)^\top \psi(y_0) / \tau}}{e^{\phi(x_0)^\top \psi(y_0) / \tau}}}], \end{aligned} \quad (2)$$

Since  $\frac{\sum_{i=1}^n e^{\phi(x_i)^\top \psi(y_0) / \tau}}{e^{\phi(x_0)^\top \psi(y_0) / \tau}}$  is usually quite small ( $< 0.1$ ) due to the exponentiation, we can taylor expand the above term around 0 and discard 2 or higher order terms, resulting in

$$\begin{aligned} \mathcal{L}_{NCE} \approx & \mathbb{E}_{x_0, y_0 \sim D} [\mathbb{E}_{y_1, \dots, y_n \sim D} \frac{\sum_{i=1}^n e^{\phi(x_0)^\top \psi(y_i) / \tau}}{e^{\phi(x_0)^\top \psi(y_0) / \tau}} \\ & + \mathbb{E}_{x_1, \dots, x_n \sim D} \frac{\sum_{i=1}^n e^{\phi(x_i)^\top \psi(y_0) / \tau}}{e^{\phi(x_0)^\top \psi(y_0) / \tau}}], \end{aligned} \quad (3)$$

which can be simplified to

$$\begin{aligned} \mathcal{L}_{NCE} \approx & n \mathbb{E}_{x_0, y_0 \sim D} [\mathbb{E}_{y_1 \sim D} e^{\phi(x_0)^\top [\psi(y_1) - \psi(y_0)] / \tau} \\ & + \mathbb{E}_{x_1 \sim D} e^{[\phi(x_1) - \phi(x_0)]^\top \psi(y_0) / \tau}]. \end{aligned} \quad (4)$$

#### 3.1.1. REDUCTION TO DOT PRODUCT

We argue that Eqn. 4 can be reduced to straightforwardly comparing the dot products. When we have no knowledge of the distribution  $D$ , the only thing that we can do is to perform a zeroth-order approximation of Eqn. 4. The most intuitive way of doing so is to reduce the distribution of  $\phi(x_1)$  and  $\psi(y_1)$  to be 0 deterministically, so that:

$$\mathcal{L}_{NCE}^{(0)} = 2n \mathbb{E}_{x_0, y_0 \sim D} e^{-\phi(x_0)^\top \psi(y_0) / \tau}. \quad (5)$$

This shows that we can essentially just output  $e^{-\phi(x_0)^\top \psi(y_0)}$  as the distance between  $x_0$  and  $y_0$ . Since in most applications, only relative comparisons of the distances matter (e.g. finding the best caption describing the image), it is the same as the negative dot product without the exponentiation.

#### 3.1.2. EFFICIENT APPROXIMATION

The common practice of taking a naive zeroth-order approximation can result in a loss of some of the important information. On the other hand, computing Eqn. 4 for each pair  $x_0, y_0$  involves iterating over all samples in a distribution  $D$ , and is computationally inefficient. We therefore turn to more efficient approximations using statistics of higher-order moments of the distribution. In our experiments, we found that this intuitive modification maintains most of the useful information as shown in Appendix 4.7.

If we know the first moment of the distribution, i.e., the mean of the unlabeled distribution  $\mu_x$  and  $\mu_y$  for  $\phi(x_1)$  and  $\psi(y_1)$ , we can perform a first-order approximation of

the distribution with  $\widehat{P}(\phi(x_1)) = \mathbb{I}\{\phi(x_1) = \mu_x\}$  and  $\widehat{P}(\psi(y_1)) = \mathbb{I}\{\psi(y_1) = \mu_y\}$ , so that  $\widehat{P}(\phi(x_1)), \widehat{P}(\psi(y_1))$  matches the true distribution in terms of the first-order moment. This simplifies Eqn. 4 to be:

$$\begin{aligned} \mathcal{L}_{NCE}^{(1)} = \\ \mathbb{E}_{x_0, y_0 \sim D} [e^{\phi(x_0)^\top (\mu_y - \psi(y_0)) / \tau} + e^{(\mu_x - \phi(x_0))^\top \psi(y_0) / \tau}]. \end{aligned} \quad (6)$$

Therefore, to evaluate the distance of any  $x_0, y_0$ , we can simply output  $e^{\phi(x_0)^\top (\mu_y - \psi(y_0)) / \tau} + e^{(\mu_x - \phi(x_0))^\top \psi(y_0) / \tau}$  without having to calculate an expectation by iterating through all samples in the distribution.

### 3.2. Effortless Implementation as Distribution Normalization

In our preliminary experiments, we found that  $e^{\phi(x_0)^\top (\mu_y - \psi(y_0)) / \tau} + e^{(\mu_x - \phi(x_0))^\top \psi(y_0) / \tau}$  correlates well with the simpler form  $-(\phi(x_0) - \frac{1}{2}\mu_x)^\top (\psi(y_0) - \frac{1}{2}\mu_y)$  after removing the exponentiation, which now introduces a constant coefficient of 0.5 to the means. For more flexibility, we replace it with  $\lambda$  so that it can be set empirically, and define the new similarity measure as:

$$S(x_0, y_0) = (\phi(x_0) - \lambda\mu_x)^\top (\psi(y_0) - \lambda\mu_y). \quad (7)$$

In all our experiments, we fix  $\lambda = 0.25$  as we found that to be the optimal value empirically. Note that the new similarity measure is equivalent to subtracting the means immediately after the original representations are calculated, a method we call Distribution Normalization (DN), after which the similarity is just their dot product. Clearly, our proposal is extremely easy to implement when access to the mean of the distribution of interest is available.

Fortunately, we observed that the mean of the distribution can usually be robustly estimated from very few unlabeled samples as shown in Section 4.6.1. This is easily accessible in all the downstream tasks that we have considered in this paper and is much cheaper than fine-tuning where not only more data is required but also the data needs to be annotated. For example, in the task of cross-modal retrieval, the mean can be estimated from the gallery data and past queries (without knowing the correct answer to the queries); in the task of zero-shot classification, the mean can be estimated from a small and unlabeled validation set; and in the task of image caption metrics, the mean can be estimated from the images to be captioned and the references provided.

## 4. Experiments

Our experiments are designed to answer the following questions: 1) whether our proposed DN can uniformly improve a wide range of cross-modal alignment tasks for different

kinds of cross-modal representation models, 2) how robust DN is when only scarce, unlabeled data is available to estimate the mean from, and 3) whether DN can improve the performance of fine-tuned models in addition to pre-trained models.

### 4.1. Downstream Tasks

**Cross-modal Retrieval** includes two subtasks where images are used to query corresponding text and vice versa. Following (Yang et al., 2022; Li et al., 2021), for each subtask, we consider both the zero-shot setting and the fine-tuning setting on COCO (Lin et al., 2014) and Flickr30K (Plummer et al., 2015). In the zero-shot setting, we directly apply the pre-trained model on the test set of each dataset while in the fine-tuned setting we first fine-tune each pre-trained model on the training set of each dataset with the InfoNCE loss and apply the fine-tuned model to the test set. For each setting, we report Recall@k ( $k = 1, 5$ ) whereby the retrieval is considered a success if its corresponding image/text is in the top-k.

**Zero-shot Classification** is the task where we directly apply the pre-trained models to predict the category of the images in the test set. Each class is represented with a fixed textual template of “a photo of {class\\_name}.”, and the corresponding representation is obtained by encoding those sentences with the text encoder of the pre-trained model. For each image, we encode it with the image encoder and output the top-k most similar class representations as predictions. We benchmark all methods with top-1 and top-5 accuracy on ImageNet1K (Deng et al., 2009), Cifar100 (Krizhevsky, 2009), SUN397 (Xiao et al., 2010), and Stanford Cars (Krause et al., 2013) datasets.

**Image Captioning Metric** is the task that measures the correlation between human ratings and similarity metrics on machine-generated captions. Following (Hessel et al., 2021), we consider both the reference-free setting and the reference-based setting. In the reference-free setting, the metric does not have access to human-written example captions (references) and has to give a score based on the source image and the generated caption alone while in the reference-based setting the metric can additionally take advantage of the information from the provided references.

### 4.2. Base Representation Models

This paper examines the effect of a Distribution Normalization layer on the following state-of-the-art open-sourced cross-modal representation models:

**CLIP** (Radford et al., 2021) is one of the earliest pioneers that successfully created a joint representation space of images and text through large-scale contrastive learning. It is trained on over 400M image-caption pairs collected by

the authors. They have open-sourced multiple versions of pretrained models and this paper examines the commonly used version "ViT-B/32".

**ALBEF** (Li et al., 2021) is one of the later variants of CLIP that adds a multi-modal encoder to capture the interplay between images and text by predicting if they are paired samples or hard negatives. Additional momentum distillation loss and masked language modeling loss are also added to improve the model performance. Two versions of pre-trained models trained on dataset consisting of 4M and 14M unique images are released and this work uses the latter. To focus on the effect of DN on cross-modal representations, we only keep the image and text encoder component of ALBEF and do not use the multi-modal encoder component.

**TCL** (Yang et al., 2022) is another state-of-the-art CLIP variant. It inherits the same model architecture as ALBEF, but adds triplet contrastive loss including Cross-modal Alignment, Intra-modal Contrastive, and Local MI Maximization. Their model is trained on 4M unique images. As with ALBEF, we only keep the image and the text encoder component.

### 4.3. Cross-modal Retrieval Results

We conducted experiments on both image-to-text and text-to-image retrieval on Microsoft COCO (Lin et al., 2014) and Flickr30K (Plummer et al., 2015) (see Appendix A.1 for datasets details). For all the retrieval tasks, we estimated the mean with 100 random unlabeled samples from the validation set and calculated standard deviations and average recalls with 5 random seeds.

The results for both datasets are presented in Table 1 for the zero-shot setting. For all three base models, adding DN almost always improves recall for both zero-shot image-to-text and text-to-image retrieval tasks, with an average 1.1% increase in top-1 recall. This provides substantial evidence that DN is effective for both tasks even in datasets with diverse images like MSCOCO. The improvement can be as large as a 2.2% increase in top-1 image-to-text recall as we see for CLIP on Flickr30K. We also observe that, in general, adding DN brings a larger improvement for top-1 recall than for top-5/10 recall, suggesting that DN is particularly suitable for distinguishing similar samples. We additionally report DN's effectiveness when we fine-tune the base models on target datasets as an ablation in section 4.6.2.

### 4.4. Zero-shot Classification Results

Table 2 gives the zero-shot classification results for all three base models and their variants with DN on ImageNet1K (Deng et al., 2009), Cifar100 (Krizhevsky, 2009), SUN397 (Xiao et al., 2010), and Stanford Cars (Krause et al., 2013)

(see Appendix A.2 for datasets details). In these experiments, we perform DN before the final norm normalization layer of image/text encoders. DN boosted the performance of all three base models on all four datasets, with an average 1.9% boost on top-1 classification accuracy. Our DN method displays great robustness as it brings performance boost in 11 out of all 12 model-dataset combinations in Table 2. Our results show that DN is effective in not only general-purpose vision datasets such as the ImageNet but also special-purpose datasets like the Stanford Cars, where the models still get (on average) 0.5% increase in accuracy. Notably, TCL saw the largest gain of 2.95% on average in top-1 accuracy and 3.3% on average in top-5 accuracy. On ImageNet1K particularly, TCL's top-1 accuracy is improved from 20.0% to 25.1% by adding DN. We believe the fact that TCL and ALBEF are pre-trained on a smaller dataset (4M & 14M images) than CLIP (400M images) resulted in TCL and ALBEF getting a larger improvement than CLIP, as DN may have helped ease the instability when the model is not adequately trained. All these improvements are achieved with a single layer that incurs minimal computational overhead.

### 4.5. Image Captioning Metric Results

Inspired by the success of CLIPScore (Hessel et al., 2021) as a metric for image captioning, we conduct experiments to test whether DN can help various cross-modal representation models align better with human judgments. To compare the performance of different methods, we report the Kendall's  $\tau_b$  or  $\tau_c$  coefficients against human judgments on Flickr8k-expert, Flickr8k-cf (Hodosh et al., 2013) and THumb (Kasai et al., 2021) in Table 3, following the standard practice in (Hessel et al., 2021). We also report the resulting accuracy for caption-caption preferences on Pascal-50S (Rashtchian et al., 2010) in Table 4. Details about these datasets are given in appendix A.3. In the reference-based setting, for CLIP-ref, we follow (Hessel et al., 2021) in using an averaged score given by:

$$\begin{aligned} \text{CLIP-ref}(x_0, y_0) = \\ \text{H-mean}(\phi(x_0)^\top \psi(y_0), \max_{c \in R} \psi(c)^\top \psi(y_0)), \end{aligned}$$

where H-mean is the harmonic mean and  $R$  is the set of provided references. On the other hand, for a distribution normalized CLIP + DN-ref, we use a weighted algorithmic mean instead:

$$\begin{aligned} \text{CLIP + DN-ref}(x_0, y_0) = \\ \text{A-mean}(S(x_0, y_0), 0.25 * \max_{c \in R} \psi(c)^\top \psi(y_0)), \end{aligned}$$

where A-mean is the algorithmic mean,  $R$  is the set of provided references, and  $S$  is defined in Eqn. 7.

In Table 3, we report the results on Flickr8K-Expert, Flickr8K-CF, and THumb for all three base models. Some

## Distribution Normalization

	MSCOCO (5K test set)						Flickr30K (1K test set)					
	Image → Text			Text → Image			Image → Text			Text → Image		
	R@1	R@5	R@10	R@1	R@5	R@10	R@1	R@5	R@10	R@1	R@5	R@10
CLIP (Radford et al., 2021)	52.4	76.0	84.5	30.2	55.1	66.4	81.3	95.0	98.5	62.7	86.0	92.0
CLIP + DN	<b>52.9</b> ±0.1	<b>76.4</b> ±0.1	<b>84.9</b> ±0.1	<b>32.1</b> ±0.1	<b>57.4</b> ±0.0	<b>68.3</b> ±0.1	<b>83.5</b> ±0.1	<b>96.2</b> ±0.0	98.5±0.1	<b>64.8</b> ±0.2	<b>87.5</b> ±0.1	<b>93.1</b> ±0.0
TCL (Yang et al., 2022)	57.6	84.3	91.8	41.8	70.6	80.6	73.8	93.3	96.9	59.1	84.6	91.1
TCL + DN	<b>59.5</b> ±0.1	<b>85.2</b> ±0.0	<b>92.2</b> ±0.1	<b>42.7</b> ±0.0	<b>71.5</b> ±0.0	<b>81.3</b> ±0.0	<b>75.5</b> ±0.0	<b>94.4</b> ±0.1	96.9±0.1	<b>60.0</b> ±0.1	<b>85.1</b> ±0.0	91.1±0.0
ALBEF (Li et al., 2021)	62.5	85.9	92.2	40.2	68.4	78.9	78.2	95.5	97.9	59.9	84.8	90.6
ALBEF+DN	<b>63.0</b> ±0.1	<b>86.0</b> ±0.0	<b>92.5</b> ±0.1	<b>42.8</b> ±0.1	<b>70.8</b> ±0.0	<b>80.7</b> ±0.0	<b>79.2</b> ±0.1	<b>96.2</b> ±0.0	<b>98.0</b> ±0.0	<b>62.4</b> ±0.1	<b>86.1</b> ±0.1	<b>91.9</b> ±0.1

Table 1. Cross-modal retrieval performance on MSCOCO and Flickr30K in the zero-shot setting. Means for DN are estimated using 100 random unlabeled validation samples. Average recalls and standard deviations are calculated with 5 random seeds.

	ImageNet1K		Cifar100		SUN397		Stanford Cars	
	Acc@1	Acc@5	Acc@1	Acc@5	Acc@1	Acc@5	Acc@1	Acc@5
CLIP (Radford et al., 2021)	61.0	87.4	63.9	88.7	56.1	89.4	58.6	<b>90.9</b>
CLIP + DN	<b>61.7</b> ±0.1	<b>87.8</b> ±0.0	<b>65.1</b> ±0.1	<b>89.4</b> ±0.0	<b>57.3</b> ±0.0	<b>90.2</b> ±0.1	<b>58.6</b> ±0.1	90.7±0.0
TCL (Yang et al., 2022)	20.0	42.9	39.1	68.2	28.6	63.4	2.0	8.7
TCL + DN	<b>25.1</b> ±0.1	<b>48.9</b> ±0.2	<b>42.2</b> ±0.0	<b>71.1</b> ±0.1	<b>31.8</b> ±0.1	<b>66.8</b> ±0.2	<b>2.4</b> ±0.0	<b>9.5</b> ±0.1
ALBEF (Li et al., 2021)	37.3	65.8	38.5	65.7	45.6	81.5	25.0	61.0
ALBEF + DN	<b>38.7</b> ±0.1	<b>67.3</b> ±0.0	<b>44.8</b> ±0.2	<b>72.0</b> ±0.2	<b>46.3</b> ±0.1	<b>82.0</b> ±0.0	<b>26.0</b> ±0.1	<b>61.7</b> ±0.2

Table 2. Zero-shot classification performance on ImageNet1K, Cifar100, SUN397 and Stanford Cars. Means for DN are estimated using 100 random unlabeled validation samples. Average accuracies and standard deviations are calculated with 5 random seeds.

methods, such as the BLEU score, are not applicable in the reference-free setting and are thus only compared with in the reference-based setting. The results strongly support that adding DN significantly improves the  $\tau$  correlation for all three base models on all dataset in the reference-free setting. In particular, CLIP + DN improves CLIP by 2.2% on Flickr8k-expert, 0.8% on Flickr8k-cf and 2.3 % on THumb. In the reference-based setting, to give a better context, we also provide the performance of other reference-based SOTA metrics that are not contrastively trained and found that CLIP and CLIP-ref outperform all of them. However, by simply adding a DN layer, CLIP-ref + DN again yields an average 1.1% gain across the board. A similar pattern is also observed in our experiment results on Pascal-50S in Table 4. Our main results on cross-modal retrieval, zero-shot classification, and image caption metrics provide extensive evidence that our proposed DN is a widely applicable modification that can improve the performance of cross-modal representation models across a variety of downstream applications.

### 4.6. Ablation Study

#### 4.6.1. NUMBER OF SAMPLES FOR MEAN ESTIMATION

We study the performance of DN when different numbers of samples are used to estimate the mean. We observe that DN consistently improves performance for CLIP, TCL, and ALBEF even when using as few as 10 unlabeled samples. Using the ImageNet1K, Cifar100, SUN397, and Stanford Cars datasets, we first test the retrieval accuracy of DN by

		Flickr8k-expert	Flickr8k-cf	THumb
		$\tau_c$	$\tau_b$	$\tau_c$
Ref-free	CLIP (Hessel et al., 2021)	51.4	34.3	19.9
	CLIP + DN	<b>53.2</b>	<b>35.1</b>	<b>22.2</b>
	TCL (Yang et al., 2022)	31.0	20.6	8.1
	TCL + DN	<b>36.0</b>	<b>23.3</b>	<b>11.1</b>
	ALBEF (Li et al., 2021)	24.9	15.4	0.9
	ALBEF + DN	<b>29.2</b>	<b>18.1</b>	<b>2.5</b>
Ref-based	BLEU-1	32.3	17.9	11.1
	BLEU-4	30.8	16.9	6.9
	CIDEr (Vedantam et al., 2014)	43.9	24.6	13.8
	NUBIA* (Kane et al., 2020)	49.5	-	-
	ViLBERTScore-F (Yi et al., 2020)	50.1	-	-
	CLIP-ref (Hessel et al., 2021)	53.0	36.4	24.7
	CLIP + DN-ref	<b>54.3</b>	<b>36.9</b>	<b>26.2</b>

Table 3. Image captioning metric results on Flickr8k-Expert, Flickr8k-CF, and THumb.

estimating the mean with the entire test set. We use the performance achieved here as an upper bound, because the mean is most reliable if it is directly calculated on the unlabeled testing samples. We compare it with the estimated means using 1, 10, and 100 random samples from the training set, and present our results in Table 5.

As shown in the table, decreasing the number of samples to just 100 from the training set results in an accuracy drop of no more than 0.2% compared to the upperbound, with an average of only 0.09%. We find that even decreasing the number of samples to as few as 10 does not significantly hurt the result. For 10 samples, there is an average drop in accuracy of 0.14%, with the greatest difference of no more than 0.4%. Moreover, for CLIP, TCL, and ALBEF, we find

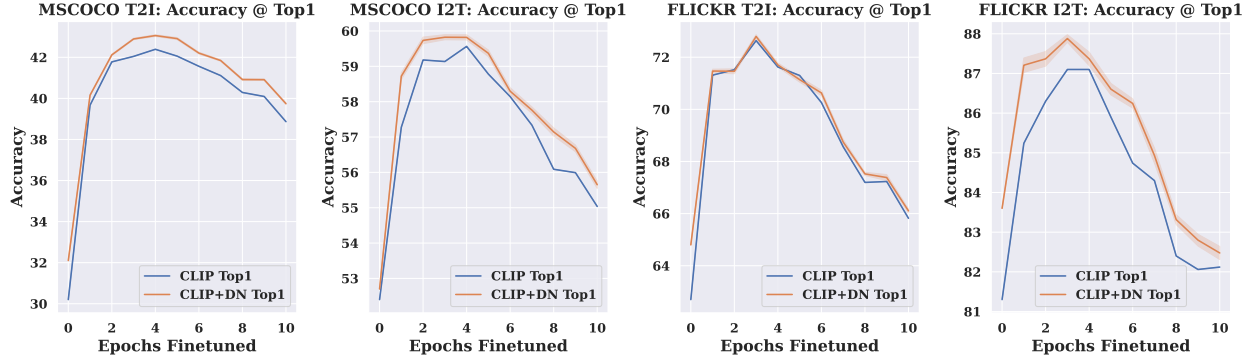


Figure 2. Comparison of the effects of fine-tuning between CLIP and CLIP + DN for Acc@1. Results on MSCOCO’s 5k test set are shown to the left, and Flickr30K’s 1k test set are shown to the right. For each set, image-to-text retrieval (left) and image-to-text retrieval (right) are reported. For each of the 5 checkpoints we trained, we find its average accuracy and standard deviation with another 5 iterations random sampling for mean estimation, and plot the mean of these 5 accuracies and standard deviations from 5 independently fine-tuned checkpoints.

	HC	HI	HM	MM	Mean
CLIP (Hessel et al., 2021)	55.0	99.2	96.9	71.8	80.7
CLIP + DN	<b>55.6</b>	<b>99.3</b>	<b>97.3</b>	<b>73.6</b>	<b>81.4</b>
TCL (Yang et al., 2022)	52.4	91.8	54.7	63.4	65.6
TCL + DN	<b>52.7</b>	<b>93.8</b>	<b>59.0</b>	<b>64.3</b>	<b>67.4</b>
ALBEF (Li et al., 2021)	56.9	98.1	<b>82.5</b>	67.2	<b>76.2</b>
ALBEF + DN	56.9	98.1	81.7	<b>67.8</b>	76.1
BLEU-4	60.4	90.6	84.9	54.7	72.6
CIDEr (Vedantam et al., 2014)	65.1	98.1	90.5	64.8	79.6
ViLBERTScore-F (Yi et al., 2020)	49.9	99.6	93.1	75.8	79.6
CLIP -ref (Hessel et al., 2021)	<b>62.4</b>	99.7	96.7	73.0	83.0
CLIP + DN -ref	61.1	99.7	<b>97.3</b>	<b>74.8</b>	<b>83.2</b>

Table 4. Accuracy results on Pascal-50S given different categories of caption-caption pairs. HC means two correct human-generated captions. HI means two human-generated captions with one incorrect. HM means a human-generated and a machine-generated caption. MM means two machine-generated captions.

that estimating the mean with as few as 10 samples still improved accuracy over the base model by an average of 1.96% for Acc@1, and 1.92% for Acc@5. Furthermore, our results are generally stable despite the low number of sample points used to estimate the mean. Across 5 random samplings, the standard deviation of our accuracy is on average 0.08% for 100 training set samples, and 0.22% for 10 training set samples. Even in the pathological case of just 1 sample, we still observe a slight improvement of 1.15% over the base model averaged across Acc@1 and Acc@5, but with a slightly larger standard deviation of 0.77%. These ablation results show that DN can generalize very well even in the setting of extremely scarce data, possibly because DN does not overfit to the unlabeled data.

#### 4.6.2. EFFECT OF FINE-TUNING ON THE RESULTS

We also perform ablations on the effects of DN on fine-tuned models. We fine-tune CLIP on the MSCOCO training set, for a total of 10 epochs on 4 Nvidia 2080Ti. We use the

Adam optimizer with a learning rate of 1e-5 and a weight decay of 0.1. We then evaluated each checkpoint on the same MSCOCO test split used in Table 1, and estimate the mean for CLIP + DN using 100 randomly sampled validation points. A total of 5 checkpoints were trained, and we evaluated each checkpoint for 5 iterations. For each checkpoint, we calculate the average accuracy and standard deviation, then plot the mean of the accuracies and standard deviations over all 5 checkpoints. We repeat this process for Flickr30K, using the same number of epochs, checkpoints, and model of GPUs. We again use the Adam optimizer with a learning rate of 1e-5, but with a weight decay of 0.02. We record accuracy scores at 1, 5, and 10 for both image-to-text retrieval and text-to-image retrieval on the two datasets. We present Acc@1 here, and leave Acc@5 and Acc@10 in Appendix B.1.

The following analysis focuses specifically on the case of Acc@1 for MSCOCO, but the general trend is also present in Flickr30K. As seen in Figure 2, fine-tuning allows for an improvement in accuracy over the zero-shot setting initially by 8.06% and 9.47% for CLIP + DN and CLIP respectively in the text-to-image case, and 6.02% and 4.88% in the image-to-text case in the first epochs. But the fine-tuning performance gradually decays after that due to overfitting to the training set. At their highest peak, CLIP + DN achieves 43.06% accuracy compared to CLIP’s 42.39% for text-to-image retrieval, and 59.82% compared to 59.57% for image-to-text retrieval. We observe for both image-to-text retrieval and text-to-image retrieval that CLIP + DN performs better than CLIP across all fine-tuning epochs by an average of 0.80% for text-to-image, and 0.60% for image-to-text case.

A similar pattern is observed in Flickr30K. At their respective peaks, CLIP + DN achieves 72.80% accuracy compared to CLIP’s 72.64% for text-to-image retrieval, and 87.88%

## Distribution Normalization

	ImageNet1K		Cifar100		SUN397		Stanford Cars	
CLIP (Radford et al., 2021)	Acc@1	Acc@5	Acc@1	Acc@5	Acc@1	Acc@5	Acc@1	Acc@5
	61.0	87.4	63.9	88.7	56.1	89.4	58.6	90.9
	61.8	87.9	65.1	89.4	57.3	90.1	58.7	90.7
	61.7 ± 0.0	87.8 ± 0.0	65.1 ± 0.1	89.4 ± 0.0	57.3 ± 0.0	90.2 ± 0.1	58.6 ± 0.1	90.7 ± 0.0
	61.6 ± 0.1	87.8 ± 0.1	65.1 ± 0.2	89.2 ± 0.1	57.1 ± 0.1	90.1 ± 0.1	58.3 ± 0.1	90.7 ± 0.1
CLIP + DN (1)	60.6 ± 0.4	87.2 ± 0.2	64.1 ± 0.6	88.4 ± 0.6	56.9 ± 0.5	89.7 ± 0.2	56.5 ± 0.4	89.7 ± 0.5
	20.0	42.9	39.1	68.2	28.6	63.4	2.0	8.7
	25.4	49.4	42.2	71.1	31.9	66.9	2.4	9.5
	25.1 ± 0.1	48.9 ± 0.2	42.2 ± 0.0	71.1 ± 0.1	31.8 ± 0.1	66.8 ± 0.2	2.4 ± 0.0	9.5 ± 0.1
	25.3 ± 0.1	49.1 ± 0.2	42.2 ± 0.2	70.9 ± 0.1	31.9 ± 0.4	66.8 ± 0.5	2.3 ± 0.1	9.5 ± 0.0
TCL (Yang et al., 2022)	25.5 ± 0.3	49.2 ± 0.3	40.8 ± 0.7	69.4 ± 0.9	31.4 ± 0.5	65.8 ± 0.9	2.3 ± 0.1	9.5 ± 0.3
	37.3	65.8	38.5	65.7	45.6	81.5	25.0	61.0
	38.7	67.4	45.0	72.1	46.2	81.9	26.0	61.8
	38.7 ± 0.1	67.3 ± 0.0	44.8 ± 0.2	72.0 ± 0.2	46.3 ± 0.1	82.0 ± 0.0	26.0 ± 0.1	61.7 ± 0.2
	38.7 ± 0.1	67.3 ± 0.1	45.1 ± 0.6	72.2 ± 0.5	45.9 ± 0.3	81.7 ± 0.2	25.8 ± 0.3	61.3 ± 0.6
ALBEF (Li et al., 2021)	37.3 ± 1.2	65.6 ± 1.4	44.3 ± 2.8	71.1 ± 3.1	45.4 ± 0.3	81.4 ± 0.6	25.0 ± 0.6	60.1 ± 1.2

Table 5. Ablation study on the effect of the number of samples to estimate the mean for ImageNet1K, Cifar100, SUN397 and Stanford Cars. Parenthesized is the number of unlabeled samples from the training set. (test) means that DN is conducted on the entire unlabeled test set. Mean and standard deviation are calculated based on 5 random samplings.

compared to 87.10% for image-to-text retrieval. On average, CLIP + DN performs better than CLIP across all fine-tuning epochs by 0.33% for text-to-image, and 1.02% for image-to-text case. Our experiments on the fine-tuning setting provide an affirmative answer to the last question we seek to answer, that DN provides a non-trivial performance boost to both pre-trained and fine-tuned cross-modal representation models.

### 4.7. Comparison of Simplified Equation and Full Equation

To investigate how much information might be lost in the process of our first-moment approximation of Eqn. 4, we carry out experiments to compare DN and its original form in Eqn. 4 and present our results in Table 6 in terms of their correlation with human judgments on image captioning datasets. Recall that in Section 3.2, we have set  $\lambda = 0.25$  based on empirical observations. To be fair, we need to also incorporate that into Eqn. 4, resulting in:

$$S(x_0, y_0) = \mathbb{E}_{y_1 \sim D} e^{\phi(x_0)^\top [0.5 * \psi(y_1) - \psi(y_0)] / \tau} + \mathbb{E}_{x_1 \sim D} e^{[0.5 * \phi(x_1) - \phi(x_0)]^\top \psi(y_0) / \tau}. \quad (8)$$

Note that this objective is extremely inefficient in practice because to calculate the similarity between every pair  $x_0, y_0$ , Eqn. 8 requires iterating over all validation samples (images and references in this case) while DN only needs to compute the mean once and does not need to access the validation samples after that. Surprisingly, in all the base models and datasets that we have studied, we did not notice any significant difference between DN and Eqn. 8 (difference < 0.1%). This shows that higher-order information contributes

negligibly to the downstream applications compared to only taking the mean, and DN provides equivalent performance without incurring expensive computational costs.

	Flickr8k-expert	Flickr8k-cf	THumb
	$\tau_c$	$\tau_b$	$\tau_c$
CLIP (Radford et al., 2021; Hessel et al., 2021)	51.4	34.3	19.9
CLIP + DN	53.2	35.1	22.2
CLIP + DN (Eqn.8)	53.2	35.1	22.2
TCL (Yang et al., 2022)	31.0	20.6	8.1
TCL + DN	36.0	23.3	11.1
TCL + DN (Eqn.8)	36.0	23.3	11.1
ALBEF (Li et al., 2021)	24.9	15.4	0.9
ALBEF + DN	29.2	18.1	2.5
ALBEF + DN (Eqn.8)	29.2	18.1	2.5

Table 6. Abaltion study on comparison with distribution normalization and full Eqn.4 on Flickr8k-Expert, Flickr8k-CF, and THumb.

## 5. Conclusion

In this paper, we identify a mismatch between the pre-training objective of cross-modal representation models like CLIP and its downstream use with a direct dot product. To address this problem, we propose Distribution Normalization (DN) that not only displays a significant advantage over direct dot product in a wide variety of settings but is also straightforward to implement. However, though being extremely sample efficient, DN still requires estimating a mean separately for each distribution and it can be of interest if a universal mean can be found so that DN is more easily applied to a wider range of downstream applications. Future research can also explore the implications of DN to the contrastive training process of cross-modal representation models.

## References

Anderson, P., Fernando, B., Johnson, M., and Gould, S. SPICE: semantic propositional image caption evaluation. *CoRR*, abs/1607.08822, 2016. URL <http://arxiv.org/abs/1607.08822>.

Banerjee, S. and Lavie, A. METEOR: An automatic metric for MT evaluation with improved correlation with human judgments. In *Proceedings of the ACL Workshop on Intrinsic and Extrinsic Evaluation Measures for Machine Translation and/or Summarization*, pp. 65–72, Ann Arbor, Michigan, June 2005. Association for Computational Linguistics. URL <https://aclanthology.org/W05-0909>.

Chen, T., Kornblith, S., Norouzi, M., and Hinton, G. E. A simple framework for contrastive learning of visual representations. *CoRR*, abs/2002.05709, 2020a. URL <https://arxiv.org/abs/2002.05709>.

Chen, T., Kornblith, S., Swersky, K., Norouzi, M., and Hinton, G. E. Big self-supervised models are strong semi-supervised learners. *CoRR*, abs/2006.10029, 2020b. URL <https://arxiv.org/abs/2006.10029>.

Chen, X., Fan, H., Girshick, R. B., and He, K. Improved baselines with momentum contrastive learning. *CoRR*, abs/2003.04297, 2020c. URL <https://arxiv.org/abs/2003.04297>.

Chen, X., Fan, H., Girshick, R. B., and He, K. Improved baselines with momentum contrastive learning. *CoRR*, abs/2003.04297, 2020d. URL <https://arxiv.org/abs/2003.04297>.

Chen, Y., Li, L., Yu, L., Kholy, A. E., Ahmed, F., Gan, Z., Cheng, Y., and Liu, J. UNITER: learning universal image-text representations. *CoRR*, abs/1909.11740, 2019. URL <https://arxiv.org/abs/1909.11740>.

Cui, Y., Yang, G., Veit, A., Huang, X., and Belongie, S. J. Learning to evaluate image captioning. *CoRR*, abs/1806.06422, 2018. URL <http://arxiv.org/abs/1806.06422>.

Deng, J., Dong, W., Socher, R., Li, L.-J., Li, K., and Fei-Fei, L. Imagenet: A large-scale hierarchical image database. In *2009 IEEE Conference on Computer Vision and Pattern Recognition*, pp. 248–255, 2009. doi: 10.1109/CVPR.2009.5206848.

Dhariwal, P. and Nichol, A. Diffusion models beat gans on image synthesis. In Ranzato, M., Beygelzimer, A., Dauphin, Y., Liang, P., and Vaughan, J. W. (eds.), *Advances in Neural Information Processing Systems*, volume 34, pp. 8780–8794. Curran Associates, Inc., 2021. URL <https://proceedings.neurips.cc/paper/2021/file/49ad23d1ec9fa4bd8d77d02681df5cfa-Paper.pdf>.

Faghri, F., Fleet, D. J., Kiros, J. R., and Fidler, S. VSE++: improved visual-semantic embeddings. *CoRR*, abs/1707.05612, 2017. URL <http://arxiv.org/abs/1707.05612>.

Gan, Z., Chen, Y., Li, L., Zhu, C., Cheng, Y., and Liu, J. Large-scale adversarial training for vision-and-language representation learning. *CoRR*, abs/2006.06195, 2020. URL <https://arxiv.org/abs/2006.06195>.

Grill, J., Strub, F., Altché, F., Tallec, C., Richemond, P. H., Buchatskaya, E., Doersch, C., Pires, B. Á., Guo, Z. D., Azar, M. G., Piot, B., Kavukcuoglu, K., Munos, R., and Valko, M. Bootstrap your own latent: A new approach to self-supervised learning. *CoRR*, abs/2006.07733, 2020. URL <https://arxiv.org/abs/2006.07733>.

He, K., Fan, H., Wu, Y., Xie, S., and Girshick, R. B. Momentum contrast for unsupervised visual representation learning. *CoRR*, abs/1911.05722, 2019. URL <http://arxiv.org/abs/1911.05722>.

Hessel, J., Holtzman, A., Forbes, M., Bras, R. L., and Choi, Y. Clipscore: A reference-free evaluation metric for image captioning. *CoRR*, abs/2104.08718, 2021. URL <https://arxiv.org/abs/2104.08718>.

Hodosh, M., Young, P., and Hockenmaier, J. Framing image description as a ranking task: Data, models and evaluation metrics. *Journal of Artificial Intelligence Research*, 47: 853–899, 2013.

Jaiswal, A., Babu, A. R., Zadeh, M. Z., Banerjee, D., and Makedon, F. A survey on contrastive self-supervised learning. *CoRR*, abs/2011.00362, 2020. URL <https://arxiv.org/abs/2011.00362>.

Jia, C., Yang, Y., Xia, Y., Chen, Y., Parekh, Z., Pham, H., Le, Q. V., Sung, Y., Li, Z., and Duerig, T. Scaling up visual and vision-language representation learning with noisy text supervision. *CoRR*, abs/2102.05918, 2021. URL <https://arxiv.org/abs/2102.05918>.

Jiang, M., Huang, Q., Zhang, L., Wang, X., Zhang, P., Gan, Z., Diesner, J., and Gao, J. Tiger: Text-to-image grounding for image caption evaluation. *CoRR*, abs/1909.02050, 2019. URL <http://arxiv.org/abs/1909.02050>.

Kane, H., Kocyigit, M. Y., Abdalla, A., Ajanoh, P., and Coulibali, M. NUBIA: NeUral based interchangeability assessor for text generation. In *Proceedings of the 1st Workshop on Evaluating NLG*

*Evaluation*, pp. 28–37, Online (Dublin, Ireland), December 2020. Association for Computational Linguistics. URL <https://aclanthology.org/2020.evalnlgeval-1.4>.

Kasai, J., Sakaguchi, K., Dunagan, L., Morrison, J., Bras, R. L., Choi, Y., and Smith, N. A. Transparent human evaluation for image captioning. *arXiv preprint arXiv:2111.08940*, 2021.

Kim, W., Son, B., and Kim, I. Vilt: Vision-and-language transformer without convolution or region supervision, 2021. URL <https://arxiv.org/abs/2102.03334>.

Krause, J., Stark, M., Deng, J., and Fei-Fei, L. 3d object representations for fine-grained categorization. In *4th International IEEE Workshop on 3D Representation and Recognition (3dRR-13)*, Sydney, Australia, 2013.

Krizhevsky, A. Learning multiple layers of features from tiny images. 2009.

Lee, H., Yoon, S., Dernoncourt, F., Kim, D. S., Bui, T., and Jung, K. ViLBERTScore: Evaluating image caption using vision-and-language BERT. In *Proceedings of the First Workshop on Evaluation and Comparison of NLP Systems*, pp. 34–39, Online, November 2020. Association for Computational Linguistics. doi: 10.18653/v1/2020.eval4nlp-1.4. URL <https://aclanthology.org/2020.eval4nlp-1.4>.

Li, G., Duan, N., Fang, Y., Jiang, D., and Zhou, M. Unicoder-vl: A universal encoder for vision and language by cross-modal pre-training. *CoRR*, abs/1908.06066, 2019. URL <http://arxiv.org/abs/1908.06066>.

Li, J., Selvaraju, R. R., Gotmare, A. D., Joty, S. R., Xiong, C., and Hoi, S. C. H. Align before fuse: Vision and language representation learning with momentum distillation. *CoRR*, abs/2107.07651, 2021. URL <https://arxiv.org/abs/2107.07651>.

Li, W., Gao, C., Niu, G., Xiao, X., Liu, H., Liu, J., Wu, H., and Wang, H. UNIMO: towards unified-modal understanding and generation via cross-modal contrastive learning. *CoRR*, abs/2012.15409, 2020a. URL <https://arxiv.org/abs/2012.15409>.

Li, X., Yin, X., Li, C., Zhang, P., Hu, X., Zhang, L., Wang, L., Hu, H., Dong, L., Wei, F., Choi, Y., and Gao, J. Oscar: Object-semantics aligned pre-training for vision-language tasks. *CoRR*, abs/2004.06165, 2020b. URL <https://arxiv.org/abs/2004.06165>.

Lin, C.-Y. ROUGE: A package for automatic evaluation of summaries. In *Text Summarization Branches Out*, pp. 74–81, Barcelona, Spain, July 2004. Association for Computational Linguistics. URL <https://aclanthology.org/W04-1013>.

Lin, T., Maire, M., Belongie, S. J., Bourdev, L. D., Girshick, R. B., Hays, J., Perona, P., Ramanan, D., Dollár, P., and Zitnick, C. L. Microsoft COCO: common objects in context. *CoRR*, abs/1405.0312, 2014. URL <http://arxiv.org/abs/1405.0312>.

Lu, X., Zhao, T., and Lee, K. Visualsparta: Sparse transformer fragment-level matching for large-scale text-to-image search. *CoRR*, abs/2101.00265, 2021. URL <https://arxiv.org/abs/2101.00265>.

Papineni, K., Roukos, S., Ward, T., and Zhu, W.-J. Bleu: a method for automatic evaluation of machine translation. In *Proceedings of the 40th annual meeting of the Association for Computational Linguistics*, pp. 311–318, 2002.

Patashnik, O., Wu, Z., Shechtman, E., Cohen-Or, D., and Lischinski, D. Styleclip: Text-driven manipulation of stylegan imagery. In *Proceedings of the IEEE/CVF International Conference on Computer Vision (ICCV)*, pp. 2085–2094, October 2021.

Peng, X., Wang, K., Zhu, Z., and You, Y. Crafting better contrastive views for siamese representation learning. *CoRR*, abs/2202.03278, 2022. URL <https://arxiv.org/abs/2202.03278>.

Plummer, B. A., Wang, L., Cervantes, C. M., Caicedo, J. C., Hockenmaier, J., and Lazebnik, S. Flickr30k entities: Collecting region-to-phrase correspondences for richer image-to-sentence models. *CoRR*, abs/1505.04870, 2015. URL <http://arxiv.org/abs/1505.04870>.

Radford, A., Kim, J. W., Hallacy, C., Ramesh, A., Goh, G., Agarwal, S., Sastry, G., Askell, A., Mishkin, P., Clark, J., Krueger, G., and Sutskever, I. Learning transferable visual models from natural language supervision. *CoRR*, abs/2103.00020, 2021. URL <https://arxiv.org/abs/2103.00020>.

Rashtchian, C., Young, P., Hodosh, M., and Hockenmaier, J. Collecting image annotations using amazon’s mechanical turk. In *Proceedings of the NAACL HLT 2010 workshop on creating speech and language data with Amazon’s Mechanical Turk*, pp. 139–147, 2010.

Robinson, J., Chuang, C., Sra, S., and Jegelka, S. Contrastive learning with hard negative samples. *CoRR*, abs/2010.04592, 2020. URL <https://arxiv.org/abs/2010.04592>.

Sohn, K. Improved deep metric learning with multi-class n-pair loss objective. In Lee, D., Sugiyama, M., Luxburg, U., Guyon, I., and Garnett, R. (eds.), *Advances in Neural Information Processing Systems*, volume 29. Curran Associates, Inc., 2016. URL <https://proceedings.neurips.cc/paper/2016/file/6b180037abbebea991d8b1232f8a8ca9-Paper.pdf>.

Tian, Y., Krishnan, D., and Isola, P. Contrastive multiview coding. *CoRR*, abs/1906.05849, 2019. URL <http://arxiv.org/abs/1906.05849>.

Tian, Y., Sun, C., Poole, B., Krishnan, D., Schmid, C., and Isola, P. What makes for good views for contrastive learning? In Larochelle, H., Ranzato, M., Hadsell, R., Balcan, M., and Lin, H. (eds.), *Advances in Neural Information Processing Systems*, volume 33, pp. 6827–6839. Curran Associates, Inc., 2020. URL <https://proceedings.neurips.cc/paper/2020/file/4c2e5eaae9152079b9e95845750bb9ab-Paper.pdf>.

van den Oord, A., Li, Y., and Vinyals, O. Representation learning with contrastive predictive coding. *CoRR*, abs/1807.03748, 2018. URL <http://arxiv.org/abs/1807.03748>.

Vedantam, R., Zitnick, C. L., and Parikh, D. Cider: Consensus-based image description evaluation. *CoRR*, abs/1411.5726, 2014. URL <http://arxiv.org/abs/1411.5726>.

Wang, H., Zhang, Y., Ji, Z., Pang, Y., and Ma, L. Consensus-aware visual-semantic embedding for image-text matching. *CoRR*, abs/2007.08883, 2020. URL <https://arxiv.org/abs/2007.08883>.

Wang, T. and Isola, P. Understanding contrastive representation learning through alignment and uniformity on the hypersphere. *CoRR*, abs/2005.10242, 2020. URL <https://arxiv.org/abs/2005.10242>.

Xiao, J., Hays, J., Ehinger, K. A., Oliva, A., and Torralba, A. Sun database: Large-scale scene recognition from abbey to zoo. In *2010 IEEE Computer Society Conference on Computer Vision and Pattern Recognition*, pp. 3485–3492, 2010. doi: 10.1109/CVPR.2010.5539970.

Yang, J., Duan, J., Tran, S., Xu, Y., Chanda, S., Chen, L., Zeng, B., Chilimbi, T., and Huang, J. Vision-language pre-training with triple contrastive learning, 2022. URL <https://arxiv.org/abs/2202.10401>.

Yi, Y., Deng, H., and Hu, J. Improving image captioning evaluation by considering inter references variance. In *Proceedings of the 58th Annual Meeting of the Association for Computational Linguistics*, pp. 985–994, Online, July 2020. Association for Computational Linguistics. doi: 10.18653/v1/2020.acl-main.93. URL <https://aclanthology.org/2020.acl-main.93>.

You, C., Zhao, R., Staib, L. H., and Duncan, J. S. Momentum contrastive voxel-wise representation learning for semi-supervised volumetric medical image segmentation. *CoRR*, abs/2105.07059, 2021. URL <https://arxiv.org/abs/2105.07059>.

Yu, J., Wang, Z., Vasudevan, V., Yeung, L., Seyedhosseini, M., and Wu, Y. Coca: Contrastive captioners are image-text foundation models, 2022. URL <https://arxiv.org/abs/2205.01917>.

Yuan, X., Lin, Z., Kuen, J., Zhang, J., Wang, Y., Maire, M., Kale, A., and Faieta, B. Multimodal contrastive training for visual representation learning. In *Proceedings of the IEEE/CVF Conference on Computer Vision and Pattern Recognition (CVPR)*, pp. 6995–7004, June 2021.

Zhai, X., Wang, X., Mustafa, B., Steiner, A., Keysers, D., Kolesnikov, A., and Beyer, L. Lit: Zero-shot transfer with locked-image text tuning. *CoRR*, abs/2111.07991, 2021. URL <https://arxiv.org/abs/2111.07991>.

Zhang, Y., Jiang, H., Miura, Y., Manning, C. D., and Langlotz, C. P. Contrastive learning of medical visual representations from paired images and text. *CoRR*, abs/2010.00747, 2020. URL <https://arxiv.org/abs/2010.00747>.

Zhou, K., Yang, J., Loy, C. C., and Liu, Z. Learning to prompt for vision-language models. *International Journal of Computer Vision*, 130(9):2337–2348, 2022.

## A. Datasets Details

There is a total of 10 datasets mentioned in this paper, as described below.

### A.1. Cross-modal Retrieval Datasets

**MSCOCO** (Lin et al., 2014) is a multi-purpose dataset known for its rich compatibility with object detection, segmentation, and image captioning tasks. It contains 118K images in its training split and more than 5K images in its test split.

**Flicker30K** (Plummer et al., 2015) is a popular benchmark for sentence-based picture portrayal. It contains 31K images with each image having five reference sentences generated by human annotators. We took a train-test split following (Yang et al., 2022) and (Li et al., 2021), which involves a selection of 30K images for fine-tuning and 1K images for testing.

### A.2. Zeroshot Classification Datasets

**ImageNet1K** (Deng et al., 2009) is the most well-known dataset for image classification that contains more than 1200K images in its training set and 100K images in its test set and covers 1000 categories of objects. Accuracy on ImageNet1K is especially widely used for evaluating state-of-the-art image classification models.

**Cifar100** (Krizhevsky, 2009) is a dataset containing 100 classes of objects, with each class having 500 training images and 100 test images.

**SUN397** (Xiao et al., 2010), the Scene UNderstanding database, contains 899 categories and about 130K images. 397 well-sampled categories are available for benchmarking state-of-the-art algorithms for scene recognition tasks.

**Stanford Cars** (Krause et al., 2013) is an image classification dataset dedicated for cars. It collects about 16K images for 196 types of cars and adopts a 50-50 train-test split. Results on Stanford Cars test our method’s effectiveness in improving special-purpose classification models.

### A.3. Image Captions Evaluation Datasets

**Flickr8K-Expert** (Hodosh et al., 2013) is a curated subset of the Flickr8K dataset that contains 17K human ratings of image-caption pairs. Each human score corresponds to one pair and is from 1 to 4 (1 means the caption is irrelevant, 4 means the caption describes the image fully correctly.)

**Flicker8K-CF** (Hodosh et al., 2013) is a similar dataset gathered from CloudFlower that contains 48K image-caption pairs and 145K binary ratings of these pairs.

**THumb** (Kasai et al., 2021) is a dataset containing some machine- and human-generated captions from the MSCOCO dataset. It has 500 images, each with 5 candidates captions that are evaluated by human annotators.

**Pascal-50S** (Rashchian et al., 2010) contains 4K caption-caption pairs with each pair describing the same image. For all pairs, annotators give a preference on which caption in the pair provides better description of the image. Caption-caption pairs are categorized based on the origins of the captions (see Table 4 for details about categories.)

## B. Additional Results

### B.1. Fine-tuning Epochs on MSCOCO and Flickr30K

In Figure 3, we present the remaining two plots of fine-tuning ablations for MSCOCO. CLIP + DN does better than CLIP by an average of 0.52% for Acc@5, and 0.37% for Acc@10. Both graphs observe a peak in accuracy around 4-5 epochs. For Acc@5, we observe an initial improvement of 9.10% for CLIP + DN after just 1 epoch, and 11.10% for CLIP on text-to-image retrieval. These respective numbers are 5.17% and 4.39% for image-to-text retrieval. For Acc@10, we observe an initial improvement of 8.53% for CLIP + DN and 10.03% for CLIP on text-to-image retrieval, and 3.14% and 3.14% respectively for image-to-text retrieval.

In Figure 4, we present the effects of finetuning on Acc@5 and Acc@10 for Flickr30K. Again, CLIP+DN does better than CLIP by an average of 0.22% for Acc@5 and 0.14% for Acc@10. All results yield a similar trend in support of the conclusion we have made in Section 4.6.2.

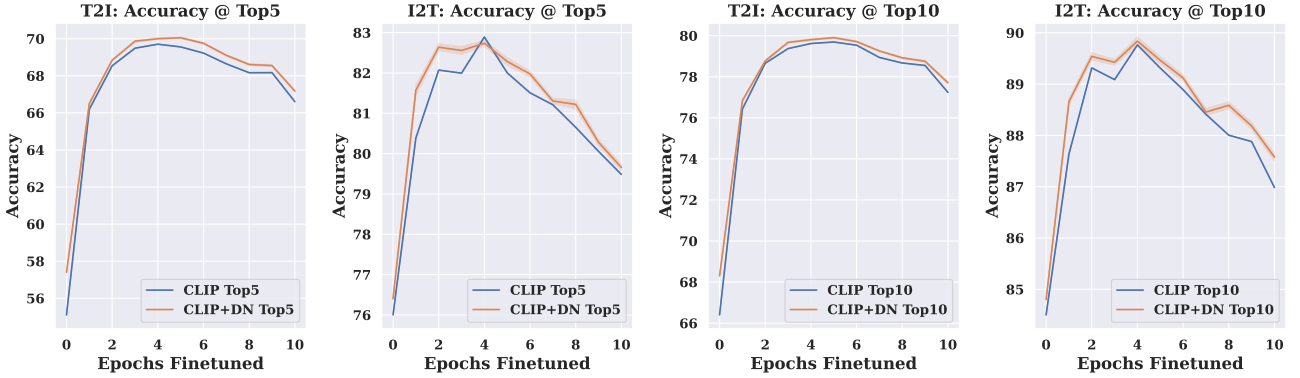


Figure 3. Comparison of the effects of fine-tuning between CLIP and CLIP + DN on MSCOCO’s 5k test set. We report text-to-image retrieval (left) and image-to-text retrieval (right) for Acc@5 and Acc@10. The average accuracy over 5 checkpoints trained with 5 random seeds is plotted. For each of the 5 checkpoints we trained, we find its average accuracy and standard deviation with another 5 iterations random sampling for mean estimation, and plot the mean of these 5 accuracies and standard deviations from 5 independently fine-tuned checkpoints.

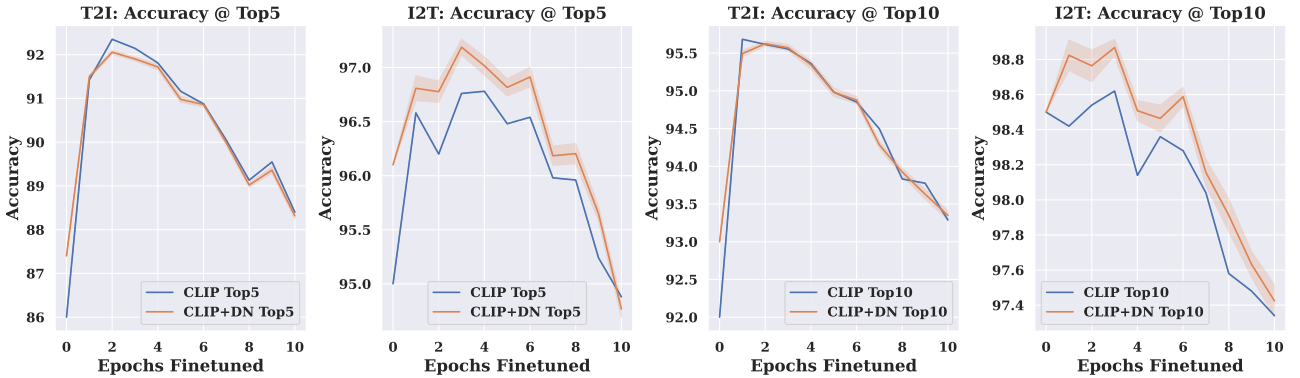


Figure 4. Comparison of the effects of fine-tuning between CLIP and CLIP + DN on Flickr30K’s 1k test set. We report text-to-image retrieval (left) and image-to-text retrieval (right) for all Acc@5 and Acc@10. The average accuracy over 5 checkpoints trained with 5 random seeds is plotted. For each of the 5 checkpoints we trained, we find its average accuracy and standard deviation with another 5 iterations random sampling for mean estimation, and plot the mean of these 5 accuracies and standard deviations from 5 independently fine-tuned checkpoints.